# 2 Density and stratification of natural waters

## 2.1 Density-relevant properties of waters

The density $\rho$ [kg m$^{-3}$] of natural waters (**oceans, estuaries, lakes, reservoirs)**, defined as the ratio of mass per volume, depends on **temperature** T and pressure p, as well as on dissolved ($C_n$; relevant are **salts, gases**) and suspended **particulate constituents** (P) in the water. In extreme cases, even isotopic compositions can influence density differences. Under natural conditions, the water column is always stratified to some extent, mostly by temperature gradients, often by salinity gradients (especially in oceans and deep lakes) and almost always by both (oceans). In fact, in lakes, ponds and reservoirs large varieties of stratifications occur. At the end of this chapter and throughout the class, you will find examples.

### a) Temperature-dependence of thermal expansivity

The **thermal expansivity** of water, $\alpha$, characterizes the temperature-dependency of density and is defined by (Figure 2.1):

**(2.1)** $$\alpha = -\rho^{-1}(\partial\rho/\partial T)_{C_{n,p}} \quad [\mathrm{K}^{-1}] \ .$$

It can be calculated from any density functions, such as Eq. (2.2) below (Figure 2.1).

Approximations for $\alpha$ are: $\alpha(T) = 10^{-6}\cdot(-\,65.4891 + 17.12544\cdot T - 0.178155\cdot T^2)$ [K$^{-1}$]
or simpler but less accurate: $\alpha(T) = 14\cdot 10^{-6}\cdot(T - 4\ °C)$ [K$^{-1}$].

With T in units [°C]. The relative density change caused by a temperature change $\Delta T$ can directly be estimated by $\Delta\rho/\rho = -\,\alpha(T)\cdot\Delta T$ [Example: T = 20 °C und $\Delta T$ = 0.1 °C; $\rightarrow \alpha(20\ °C) = 207\cdot 10^{-6}\ °C^{-1}$; and therefore $\Delta\rho/\rho = -20.7\cdot 10^{-6}$]. $\alpha(T)$ increases with warmer temperatures (Figure 2.1) and for ~4 °C (details depend on salinity S) $\alpha \rightarrow 0$ (density reaches the maximum). The temperature-dependent density, expressed by a three-order polynomial expression,

**(2.2)** $$\rho_0(T) = 999.84298 + 10^{-3}\cdot(65.4891\cdot T - 8.56272\cdot T^2 + 0.059385\cdot T^3)\ [\mathrm{kg\ m^{-3}}]$$

has been determined by Bührer and Ambühl (1975) from water density at p = 1.013 bar (sea level). It is valid for temperatures from 1 to 20 °C with a relative deviation from measured values, $\delta\rho/\rho$, of less than $2\cdot 10^{-6}$. Even simpler but less correct, is the quadratic approximation (T in [°C]), which can easily be memorized as a rule of thumb:

**(2.3)** $$\rho_0(T) \approx 1000 - 7\cdot 10^{-3}\,(T - 4\ °C)^2 \qquad [\mathrm{kg\ m^{-3}}]$$

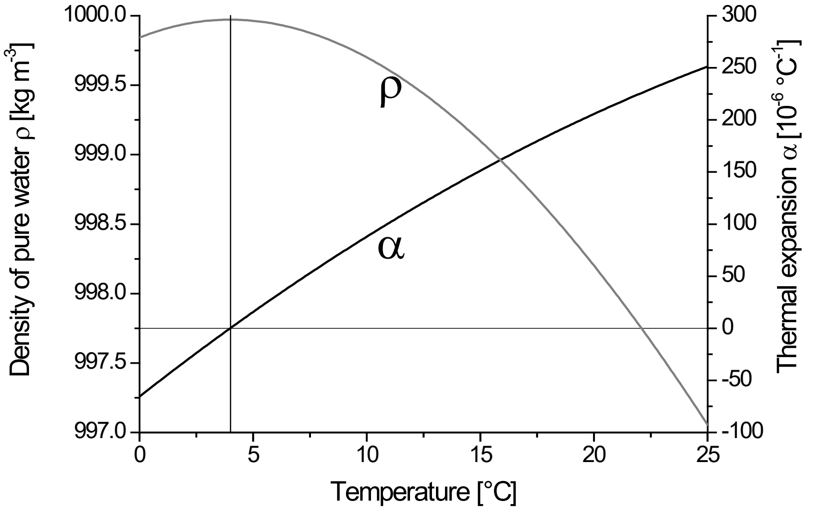

**Figure 2.1** *Density $\rho_0(T)$ und thermal expansivity $\alpha(T)$ as a function of temperature from 0 to 25 °C. Note: For $T \rightarrow 4$ °C (fine vertical line): $\rho \rightarrow$ max and therefore $\alpha \rightarrow 0$.*

## b) Freezing temperature and temperature of maximum density

Low saline water has the odd property that the densest water is not at the freezing point $T_F$, but a few °C above $T_F$. The water is densest at $T_F$ (i.e $T_F = T_{MD}$) only if it has a salinity $S > 24.695$ g kg$^{-1}$). The freezing point, being reduced by salinity and pressure p [bar], is given by (*Chen and Millero* 1986; see Figure 2.2):

**(2.4)** $T_F(S,p) = -0.0137 - 0.052 \cdot S - 0.00748 \cdot p$

Another approximation is $T_F(S,p) = T_F(S,0) - 0.000753 \cdot p$ (*Fujino et al.* 1974; *UNESCO* 1978).

The temperature $T_{MD}$ of maximum density for **low saline water** (*Chen and Millero* 1986) is:

**(2.5)** $T_{MD}(S,p) = 3.9839 - 0.019911 \cdot p - 5.822 \cdot 10^{-6} \cdot p^2 - (0.2219 + 1.106 \cdot 10^{-6} \cdot p) \cdot S$ [°C]

For atmospheric pressure (p = 0), the temperature and salinity where $T_F(S,0) = T_{MD}(S,0)$ are as follows:

$T^* = -1.33$ °C and $S^* = 24.695$ g kg$^{-1}$.

For freshwater (S = 0), $T_F(0,p)$ and $T_{MD}(0,p)$ cross at $p^* = 284$ bar (Figure 2.2). The maximum density is given by *Chen and Millero* (1986):

**(2.6)** $\rho_{MD}(S,p) = 999.972 + 4.94686 \cdot 10^{-2} \cdot p - 2.0918 \cdot 10^{-6} \cdot p^2 + (0.80357 + 1 \cdot 10^{-4} \cdot p) \cdot S$ [kg m$^{-3}$]

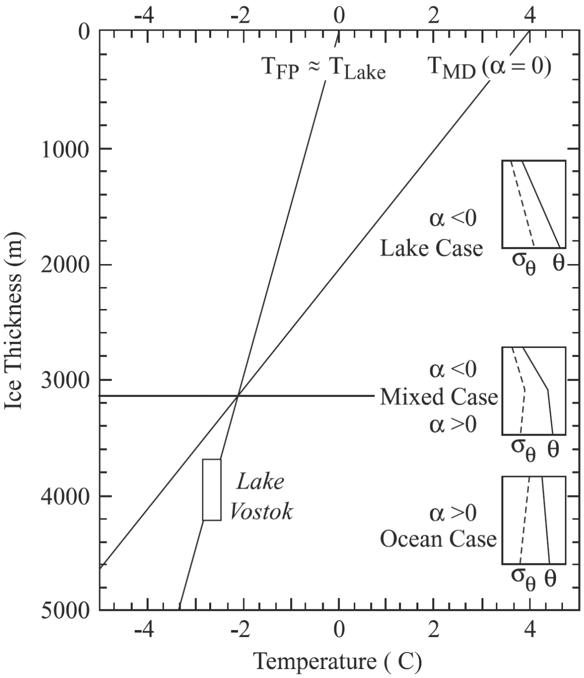

**Figure 2.2**

*Cross over of $T_F(S=0,p)$ with $T_{MD}(S=0,p)$ under ice in Antarctica at p* = 284 bar. For ice density = 913 kg $m^{-3}$ the corresponding depth is 3170 m (from Wüest and Carmack 2000).*

**Practical things to know:**

- Stratification by temperature is the most common situation in freshwater lakes. In summer and especially in the tropics, where temperature is far above temperature of maximum density ($T >> T_{MD} \approx 4$ °C for freshwater), water is commonly stably stratified due to warm water overlying cool water. In winter and especially in polar regions, where temperature sinks below temperature of maximum density ($T < T_{MD}$), water becomes stably stratified due to cool water at the surface and warmer water underneath.
- Most freshwater lakes have a typical salinity of $S \approx 0.1$ to 0.2 g $kg^{-1}$. For such waters, the temperature of maximum density is at $T_{MD}$ = 3.96 and 3.94 °C, respectively. The salt water bodies of Caspian Sea ($S \approx 13$ g $kg^{-1}$), Black Sea ($S \approx 18$ g $kg^{-1}$, surface) and Lake Van ($S \approx 22$ g $kg^{-1}$) have $T_{MD}$ at the surface of 1.10, -0.01 and -0.90 °C.
- With increasing depth, $T_{MD}$ decreases at a rate of ~2 °C per 1000 m (Figure 2.2) and Eq. (2.5). The pressure-dependence of $T_{MD}$ is relevant in all deep cold lakes such as Lake Baikal (see below), Crater Lake (see below), the Arrow Lakes (Figure 2.3) and many more.
- There are freshwater lakes ($S \approx 0$) in the ice shield of Antarctica with $T_F(S=0, p) > T_{MD}(S=0, p)$. This condition is fulfilled if p > 284 bar (i.e > 3170 m of ice), such as in Lake Vostok (Figure 2.2) and other under-ice lakes located in Eastern Antarctica (*Siegert et al.* 1996).

## c) Density effect of total dissolved solids

For freshwater one would expect that the effect of salinity is negligible. However, in temperate and polar regions, where deep-water is cool and therefore temperature is close to $T_{MD}$ (where $\alpha = 0$ by definition), even small salinity gradients contribute to the density stratification. A typical example is given in Figure 2.3 (Lake Arrow).

The **haline contraction coefficients** describe the contribution of salinity (or total dissolved solids, **TDS**) to the density, defined by:

**(2.7)** $\beta_n = \rho^{-1}(\partial\rho/\partial C_n)_{T,p,Cm}$

expressing the relative change of density per unit of salinity for the individual salts $C_n$ in solution. If sufficiently diluted (e.g. low ionic strength), the contribution of solute n = 1,2,... (with concentration $C_n$) on the density $\rho$ can be expressed by the linear superposition (Eq. (2.13, below). The coefficient $\beta_n$ is slightly temperature-dependent; values for various solutes at T = 25 °C are given in Table 2.1. For dissolved gases, $\beta_n$ can be negative, which means that the density of the water decreases with increasing gas concentration - the classical example is methane ($\beta_{CH4} = -1.25 \cdot 10^{-3}$ kg $g^{-1}$). The other important gas, $CO_2$ has a positive $\beta_{CO2} \approx 0.25 \cdot 10^{-3}$ kg $g^{-1}$ (increasing the density). For ocean water $\beta_S \approx 0.78 \cdot 10^{-3}$ kg $g^{-1}$.

**Table 2.1**
Haline contraction coefficients $\beta_n$ of different salts in lakes (*Imboden and Wüest* 1995).

| **Substance** | **$\beta_n$ (kg $g^{-1}$)** |
|---|---|
| $Ca(HCO_3)_2$ | $0.807 \cdot 10^{-3}$ |
| $Mg(HCO_3)_2$ | $0.861 \cdot 10^{-3}$ |
| $Na(HCO_3)$ | $0.727 \cdot 10^{-3}$ |
| $K(HCO_3)$ | $0.669 \cdot 10^{-3}$ |
| $Fe(HCO_3)_2$ | $0.838 \cdot 10^{-3}$ |

**Practical things to know:**

- In temperate and polar regions - where $\alpha$ is very small - salinity defines the density stratification in the deep waters (say typically below 50 m; see Figure 2.3). In freshwater lakes, TDS gradients are often due to photosynthesis / calcite precipitation (surface) and mineralization / calcite re-dissolution (deep). Details in Chapter 1.
- In salt lakes (Dead Sea, Black Sea, Lake Van, etc.) salinity is the dominant factor for density stratification (less so in the Caspian Sea), and vertical salinity gradients are mainly caused by the freshwater balance (river input versus evaporation).
- The coefficient of haline contraction $\beta$ does not vary much among different aquatic systems. For most waters, $\beta$ is within a few % equal to the value of $0.804 \cdot 10^{-3}$ kg $g^{-1}$ given by *Chen and Millero* (1986). Even for Dead Sea water (among the most saline on Earth with S ≈ 280 g $kg^{-1}$) $\beta$ deviates only a few %. In the natural waters in Switzerland, with $Ca^{2+}/HCO_3^-$ as the dominant ions, also this $\beta$ value is very close (Table 2.1).
- In some cases, the chemistry of the lake water is dominated by a single anion/cation pair, e.g. by calcium and bicarbonate. The electrical conductivity $\kappa_{20C}$ or $\kappa_{25C}$ [$\mu$S/cm] can then serve as a direct measure of the total concentration of these ions. Given their specific electrical conductivity (Chapter 1) and ionic volumes, we can obtain an expression for the dependence of $\rho$ on $\kappa_{20}$. For the case of calcium carbonate, the following relationship is obtained:

**(2.8)** $$\rho(T,\kappa_{20}) = \rho_0(T) \cdot [1 + \beta_\kappa \kappa_{20}], \text{ with } \beta_\kappa = \rho^{-1}\cdot(\partial\rho/\partial\kappa_{20}) = 0.705\cdot10^{-6}\ (\mu\text{S/cm})^{-1}$$

In practice, the salinity is determined based on conductivity (usually CTD) measurements (see Chapter 1). For a specific natural water body, the **conductivity-TDS** relation can be derived (Chapter 1). In addition the **TDS-density** relation can be calculated based on the specific salt composition (some values in Table 2.1). The procedure is described in *Wüest et al.* (1996).

## d) Density effect of suspended matter

Suspended solids (e.g. mineral particles, eroded soil, etc) – often called **total suspended sediments** (TSS) or **total suspended matter** (TSM) - also contribute to the density of water (without changing conductivity/salinity; not charged ions). Their effect therefore needs to be included as a separate term in the density estimation. The contribution of the particle concentration P [kg m$^{-3}$] to the density of the "particle-containing" water depends on the density of the particles $\rho_P$ [kg m$^{-3}$]. The contribution is:

**(2.9)** $$\Delta\rho(P) = [1 - (\rho_W/\rho_P)]\cdot P \qquad [\text{kg m}^{-3}]$$

For inorganic particles with $\rho_P$ = 2700 kg m$^{-3}$ (quartz) the relation is $\Delta\rho(P) = 0.63\cdot P$.

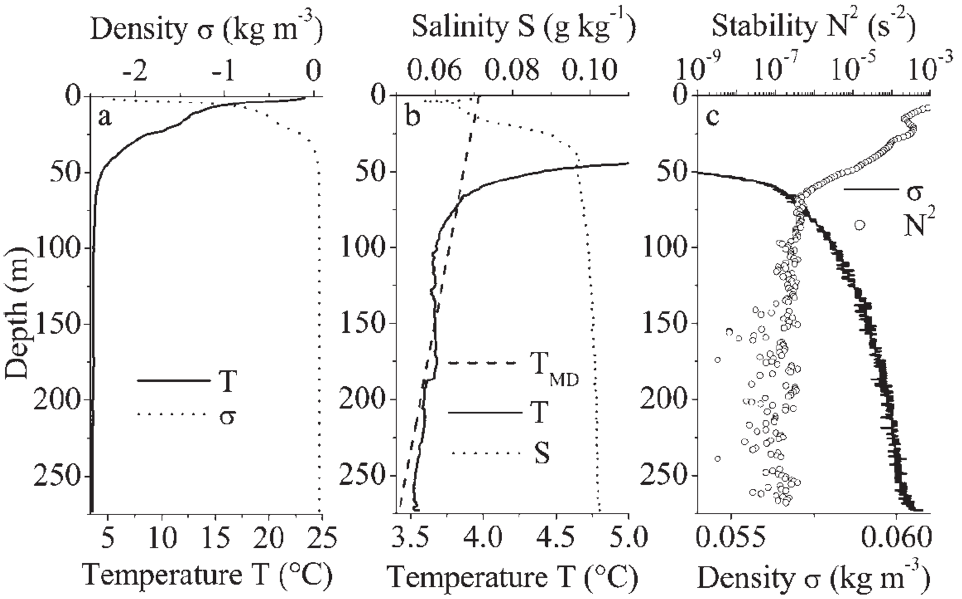

***Figure 2.3** Example of water column stratification: Temperature, salinity, and density $\rho(T,S)$ as well as stability $N^2$ (see section 2.5) as a function of depth for the Columbia Basin lake Upper Arrow on 14 August 1998 (Matzinger et al. 2007). The density profile based on temperature alone (without salinity) would not be stable (see middle panel where $T_{MD}$ indicates the pressure-dependent temperature of maximum density).*

***Sigma-units:** $\sigma(T,S) = \rho(T,S)$ - 1000 kg m$^{-3}$ (this is a convenient way to show density at a higher resolution). For the definition of stability $N^2$ see section 2.5.*

## 2.2 Equation of state of pure and low-saline water

**Formula by Chen and Millero** - The density of pure water as a function of temperature is often calculated by the equation Chen and Millero (1986), covering the limnological range ($S < 0.6$ g kg$^{-1}$; T = 0° to 30 °C, and $\rho$ = 0 to 180 bars). The equation of state has a precision of better than 2 x 10$^{-6}$ g cm$^{-3}$. The density at the surface, $\rho_{p=0}$, is given by

**(2.10)**
$$\begin{aligned}\rho_{p=0}\ (\text{g cm}^{-3}) = {} & 0.9998395 + 6.7914 \cdot 10^{-5} T - 9.0894 \cdot 10^{-6} \cdot T^2 + 1.0171 \cdot 10^{-7} \cdot T^3 \\ & - 1.2846 \cdot 10^{-9} \cdot T^4 + 1.1592 \cdot 10^{-11} \cdot T^5 - 5.0125 \cdot 10^{-14} T^6 \\ & + (8.181 \cdot 10^{-4} - 3.85 \times 10^{-6} \cdot T + 4.96 \cdot 10^{-8} \cdot T^2) \cdot S,\end{aligned}$$

where $T$ is the temperature in °C, and $S$ is the salinity in units of g kg$^{-1}$. *In-situ* density increases with pressure, given by the compressibility $K^{-1}$ of water. The density at pressure p, $\rho_p$, can be calculated from:

**(2.11)**
$$\rho_p = \rho_{p=0}\,(1 - p/K)^{-1}$$

**(2.12)**
$$\begin{aligned}K\ (\text{bar}) = {} & 19{,}652.17 + 148.113 \cdot T - 2.293 \cdot T^2 + 1.256 \cdot 10^{-2} \cdot T^3 - 4.18 \cdot 10^{-5} \cdot T^4 \\ & + (3.2726 - 2.147 \cdot 10^{-4} \cdot T + 1.128 \cdot 10^{-4} \cdot T^2) \cdot P \\ & + (53.238 - 0.313 \cdot T + 5.728 \cdot 10^{-3} \cdot p) \cdot S.\end{aligned}$$

Values for $K^{-1}$ are given in Table 2.3. The *in-situ* density is relevant if we are interested in absolute density for processes such as underwater acoustics or for the calculation of pressure from CTD profiles. For mixing and transport, the effect of compressibility on density is reversible and therefore irrelevant for stratification. Therefore, in the following, density is always calculated for pressure p = 0 (surface). The effect of compressibility on *in-situ* temperature has to be corrected for a reference at the surface (p = 0; see **potential temperature** below).

**Addition to density by low Total Dissolved Solids (salinity)** - If salinity or TDS is very low (say $S < 0.4$ g kg$^{-1}$) and the chemical composition of the TDS is known, then the contributions of the different constituents $C_i$ to the density can - as a good approximation - be added linearly by (Table 2.1):

**(2.13)**
$$\rho(T, C_1, C_2, \ldots) = \rho_o(T) \cdot [1 + \beta_1 \cdot C_1 + \beta_2 \cdot C_2 + ..]$$

If the relative chemical composition of the TDS is constant (as is nearly the case for seawater), then the influence of the different components $C_i$ can be represented by one single parameter such as the salinity S. The influence of S on $\rho$ is then described by a single ***coefficient of haline contraction*** $\beta_S$, as follows:

**(2.14)**
$$\rho(T,S) = \rho_o(T) \cdot [1 + \beta_S S], \text{ with } \beta_S = \rho^{-1} \cdot (\partial\rho/\partial S)_{T,p}$$

**Table 2.2** Thermal expansivity ($10^{-6}$ $K^{-1}$) of pure water at various T and p (Chen Millero, 1986).

| P | t (°C) | | | | | | |
|---|---|---|---|---|---|---|---|
| (bars) | 0 | 5 | 10 | 15 | 20 | 25 | 30 |
| 0 | −68.00 | 15.96 | 87.99 | 150.89 | 206.76 | 257.17 | 303.24 |
| 10 | −64.32 | 18.93 | 90.35 | 152.72 | 208.17 | 258.25 | 304.08 |
| 20 | −60.64 | 21.90 | 92.70 | 154.55 | 209.58 | 259.33 | 304.92 |
| 30 | −56.95 | 24.87 | 95.05 | 156.39 | 210.98 | 260.40 | 305.76 |
| 40 | −53.27 | 27.84 | 97.41 | 158.22 | 212.39 | 261.48 | 306.60 |
| 50 | −49.59 | 30.81 | 99.76 | 160.05 | 213.79 | 262.55 | 307.44 |
| 60 | −45.91 | 33.78 | 102.11 | 161.88 | 215.20 | 263.63 | 308.28 |
| 80 | −38.54 | 39.72 | 106.82 | 165.54 | 218.01 | 265.78 | 309.96 |
| 100 | −31.18 | 45.66 | 111.52 | 169.21 | 220.82 | 267.93 | 311.65 |
| 140 | −16.45 | 57.54 | 120.94 | 176.53 | 226.45 | 272.23 | 315.01 |
| 180 | −1.72 | 69.42 | 130.35 | 183.86 | 232.07 | 276.54 | 318.37 |

**Table 2.3** Isothermal compressibility ($10^{-6}$ $bar^{-1}$) of pure water at various temperatures and pressures (Chen and Millero, 1986).

| P | t (°C) | | | | | | |
|---|---|---|---|---|---|---|---|
| (bars) | 0 | 5 | 10 | 15 | 20 | 25 | 30 |
| 0 | 50.89 | 49.17 | 47.81 | 46.73 | 45.89 | 45.25 | 44.77 |
| 10 | 50.74 | 49.04 | 47.68 | 46.61 | 45.77 | 45.13 | 44.65 |
| 20 | 50.60 | 48.90 | 47.55 | 46.49 | 45.66 | 45.02 | 44.54 |
| 30 | 50.45 | 48.77 | 47.43 | 46.37 | 45.54 | 44.90 | 44.42 |
| 40 | 50.31 | 48.63 | 47.30 | 46.25 | 45.42 | 44.79 | 44.31 |
| 50 | 50.17 | 48.50 | 47.18 | 46.13 | 45.31 | 44.67 | 44.19 |
| 60 | 50.03 | 48.37 | 47.05 | 46.01 | 45.19 | 44.56 | 44.08 |
| 80 | 49.74 | 48.10 | 46.80 | 45.77 | 44.96 | 44.33 | 43.85 |
| 100 | 49.46 | 47.84 | 46.55 | 45.54 | 44.73 | 44.11 | 43.63 |
| 140 | 48.90 | 47.32 | 46.07 | 45.07 | 44.28 | 43.66 | 43.18 |
| 180 | 48.35 | 46.81 | 45.58 | 44.61 | 43.84 | 43.22 | 42.74 |

**Table 2.4** Specific heat at constant pressure ($J\ g^{-1}\ K^{-1}$) for pure water at various temperatures and pressures (Chen and Millero, 1986).

| P | t (°C) | | | | | | |
|---|---|---|---|---|---|---|---|
| (bars) | 0 | 5 | 10 | 15 | 20 | 25 | 30 |
| 0 | 4.2174 | 4.2021 | 4.1919 | 4.1853 | 4.1814 | 4.1793 | 4.1783 |
| 10 | 4.2125 | 4.1978 | 4.1881 | 4.1819 | 4.1783 | 4.1764 | 4.1754 |
| 20 | 4.2076 | 4.1936 | 4.1843 | 4.1786 | 4.1753 | 4.1735 | 4.1726 |
| 30 | 4.2028 | 4.1893 | 4.1806 | 4.1753 | 4.1722 | 4.1706 | 4.1698 |
| 40 | 4.1980 | 4.1851 | 4.1769 | 4.1720 | 4.1692 | 4.1678 | 4.1670 |
| 50 | 4.1932 | 4.1810 | 4.1732 | 4.1687 | 4.1662 | 4.1650 | 4.1643 |
| 60 | 4.1884 | 4.1768 | 4.1696 | 4.1654 | 4.1633 | 4.1622 | 4.1616 |
| 80 | 4.1790 | 4.1686 | 4.1624 | 4.1591 | 4.1575 | 4.1567 | 4.1563 |
| 100 | 4.1697 | 4.1606 | 4.1554 | 4.1528 | 4.1518 | 4.1514 | 4.1511 |
| 140 | 4.1515 | 4.1448 | 4.1416 | 4.1406 | 4.1407 | 4.1411 | 4.1410 |
| 180 | 4.1338 | 4.1295 | 4.1283 | 4.1289 | 4.1302 | 4.1312 | 4.1315 |

## 2.3 Potential temperature

The *in-situ* temperature is modified by thermal expansivity $\alpha$ and the pressure p and it deviates from the "***potential temperature***" that a water parcel would have if virtually displaced to p = 0 (to the surface). This is a well-known phenomenon in air (when hiking down from a mountain you feel the warming of ~6 °C / 1000 m elevation). In water this ***adiabatic*** correction is strongest for high temperatures and is most relevant for water bodies with very small temperature gradients, as the correction depends via $\alpha$ on the absolute temperature but not on the gradients. It implies that the adiabatic correction is most important in deep tropical waters such as Lake Tanganyika, Lake Malawi, etc. An example, showing the difference between *in-situ* and potential temperature is given in Figure 2.4.

The adiabatic lapse rate, $\Gamma$, i.e. the rate of increase of *in-situ* temperature T with depth caused by isentropic compression of water, is given by the thermodynamic equation:

**(2.15)**
$$\Gamma(T,p,S) = \frac{g\alpha}{C_p}(T + 273.15\ K) \qquad [\mathrm{K\ m^{-1}}]$$

where $g = 9.81\ \mathrm{m\ s^{-2}}$ is the acceleration of gravity, $\alpha = -\rho^{-1}\cdot(\partial\rho/\partial T)$ $[\mathrm{K^{-1}}]$ the thermal expansivity, $c_p$ $[\mathrm{J\ kg^{-1}\ K^{-1}}]$ the specific heat at constant pressure and T [°C] + 273.15 K is the absolute temperature. The two parameters $\alpha$ and $c_p$, which are functions of T, p and S, are calculated from Chen and Millero's (1986) equations. With respect to a reference depth of $z_O$ (here $z_O = 0$ m = lake surface), the potential temperature, $\theta(z,z_O)$, of a water parcel at depth z (positive upwards), is defined as the temperature of that water parcel if it were to be displaced isentropically from z to $z_O$:

**(2.16)**
$$\theta(z,z_O) = T(z) - \int_z^{z_O} \Gamma(\theta(z;z');p(z');S(z))\ dz' \qquad [^\circ\mathrm{C}]$$

Polynomial expressions for $\theta(T(z),p(z),S(z),z_O)$, provided by Bryden (1973), are valid only for the range of seawater salinities. Thus, for freshwater, we solve eq. 2.16 iteratively by the procedure:

**(2.17)**
$$\theta^{(0)}(z,z_O) = T(z) \text{ and } \theta^{(i+1)}(z,z_O) = T(z) - \int_z^{z_O} \Gamma(\theta^{(i)}(z;z');p(z');S(z))\ dz' \quad [^\circ\mathrm{C}\ ]$$

which converges well enough after 2 iterations ($|\theta^{(2)} - \theta^{(3)}| < 10^{-4}$ °C). In warm waters, the adiabatic correction (integral term) is positive ($\Gamma > 0$) and, consequently, $\theta < T$. The differences between *in-situ* and potential temperature in Lake Malawi (up to 0.12 °C; Figure 2.4) are significantly larger than in temperate lakes. This is due to the high thermal expansivity $\alpha$ of warm water (eq. 2.15). The minimum *in-situ* temperature occurs at a depth of approximately 400 m, below which the *in-situ* temperature gradually increases (Figure 2.4), whereas the minimum potential temperature is reached close to the deepest layers of the lake (details in Figure 2.4).

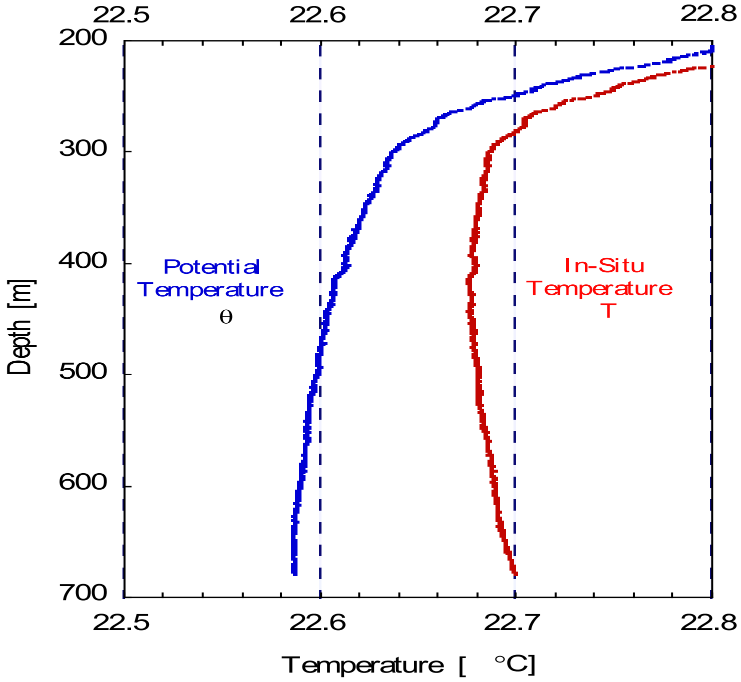

***Figure 2.4** In-situ temperature (red), T, and potential temperature (blue), $\theta$, as a function of depth in Lake Malawi. At the deepest point, the potential temperature is ~0.12 °C cooler than the in-situ T. Most important, the vertical gradient indicates that temperature is stabilizing the whole water column (except in the bottom boundary layer, where geothermal heat from the earth's interior and bottom boundary mixing homogenize a 40 m thick bottom layer; constant within 0.001 °C). This stabilizing, $N^2 > 0$, is only evident from the potential temperature but not from in-situ T.*

**Practical things to know:**

- In the ocean, $\alpha$ is not varying strongly in deep waters and therefore the adiabatic lapse rate $\Gamma$ is almost ~constant. The correction from *in-situ* to potential temperature is ~0.1 K per 1000 m depth (or ~1 K at the greatest depth of ~10 km of the ocean; Mindanao Trench).
- For $\alpha = 0$, the correction vanishes and therefore for cool waters of great depth (such as Lake Baikal or Upper Arrow (Figure 2.3), the differences between *in-situ* T and potential $\theta$ are usually negligible.
- In deep tropical waters, the transformation to potential temperature is necessary, as it is in the order of 0.1 K per 600 m depth (see example in Figure 2.4) and more than the *in-situ* temperature variations.

## 2.4 Water-column stability

### a) Definition

The strength of the stratification of a water column is expressed in terms of the intrinsic buoyancy frequency N, which a parcel experiences in a stratification $\rho(z)$. The **stability** $N^2$ is given by

$$\textbf{(2.18)} \qquad N^2 = -\left(\frac{g}{\rho} \cdot \frac{\partial \rho}{\partial z}\right) = g \cdot \left[\alpha \cdot \left(\frac{\partial T}{\partial z} - \Gamma\right) - \beta_S \cdot \frac{\partial S}{\partial z}\right] = g \cdot \left(\alpha \frac{\partial \Theta}{\partial z} - \beta_S \frac{\partial S}{\partial z} + ..\right) \qquad [s^{-2}]$$

where g = gravitational acceleration, $\rho$ = potential density, z = vertical coordinate (positive upward), $\alpha$ = thermal expansivity, $\beta_S$ = haline contraction coefficient, $\Theta$ = potential temperature and S = salinity. Besides the temperature and the salinity term, additional terms may become relevant, when (i) stability is very low (e.g. gradient of gases, such as $CO_2$ or $CH_4$, or silica in deep lakes), or when (ii) inflowing river water or bottom boundary water contains high particle concentrations.

$N^2$ varies over ~10 orders of magnitude in natural waters from ~$10^{-11}$ $s^{-2}$ (in well-mixed bottom layers or double-diffusive layers; arctic Canada Basin) to ~1 $s^{-2}$ in extreme haloclines (merging fresh and salt water; Baltic Sea; and top of salt lakes).

$N^2 > 0$ indicates stable stratification; $N^2 = 0$ is neutral stratification; $N^2 < 0$ indicates unstable stratification. The latter can occur in natural waters only locally, such as in a river mouth (delta region), in deep intruding river water parcels, in the convective surface layer (e.g. cooling at night) or within a turbulent eddy. In all other water volumes, the stability is positive (stable) otherwise the water layer would restratify until the water column is stable again.

The definition of N [$s^{-1}$] (including g and $\rho$) is such that it corresponds with the eigen-frequency of the harmonic oscillator related to a water parcel bouncing up-down relative to its equilibrium position in the stratification $\rho(z)$.

### b) Biogenic density stratification

In low-saline waters, biogeochemical processes, such as photosynthesis and subsequent settling of biogenic particles and mineralization by bacteria, may significantly change (generally enhance) vertical salinity gradients and thereby increase the *stability* $N^2$ of the water column (see Chapter 1). This phenomenon, common in many deep and eutrophic lakes (especially close to the sediment) is usually the cause of permanent density stratification (so-called *meromixis*). $Ca^{2+}$ and $HCO_3^-$ are often the dominant ions for biogenic stratification (Chapter 1).

The term **meromixis** refers to a natural water body, which does not experience deep convective mixing (due to winter cooling). Meromixis is mostly linked to permanent salinity gradients at greater depth (see example of Powell Lake; Chapter 1). Examples are Lakes Tanganyika, Malawi, Kivu, but also shallow lakes with sub-aquatic salt-containing inflows (Lago Cadagno) as well as eutrophic lakes. Meromixis can however also occur in deep lakes, where pressure changes the temperature of maximum density so much that it becomes relevant for the annual temperature dynamics (see Lake Baikal as the classical example).

## 2.5 Examples of stratification in lakes and reservoirs

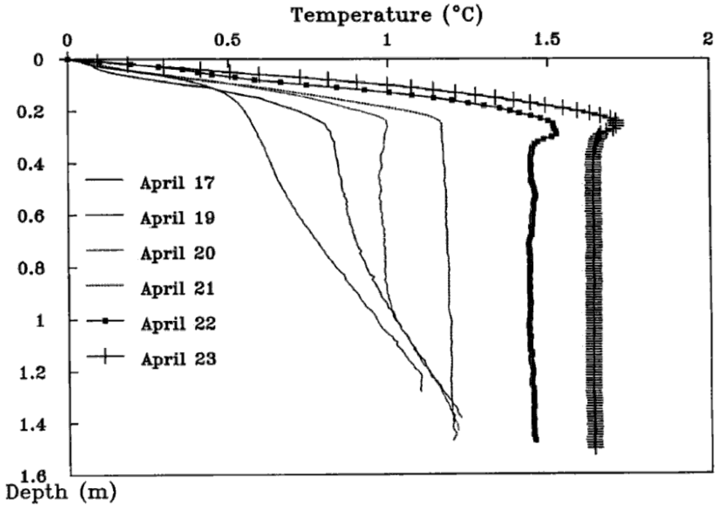

Fig. 10. Temperature development beneath the ice at Sta. 4–3 during 17–23 April.

***Figure 2.5*** *Temperature stratification under ice. Some of the sunlight is penetrating through ice and is warming the water underneath. For* $T < T_{MD}$ *the warming causes denser water which leads to convection. The convection is very clearly visible in the profiles of 22/23 April between 0.4 and 1.4 m depth. Source: Malm, et al. 1998.*

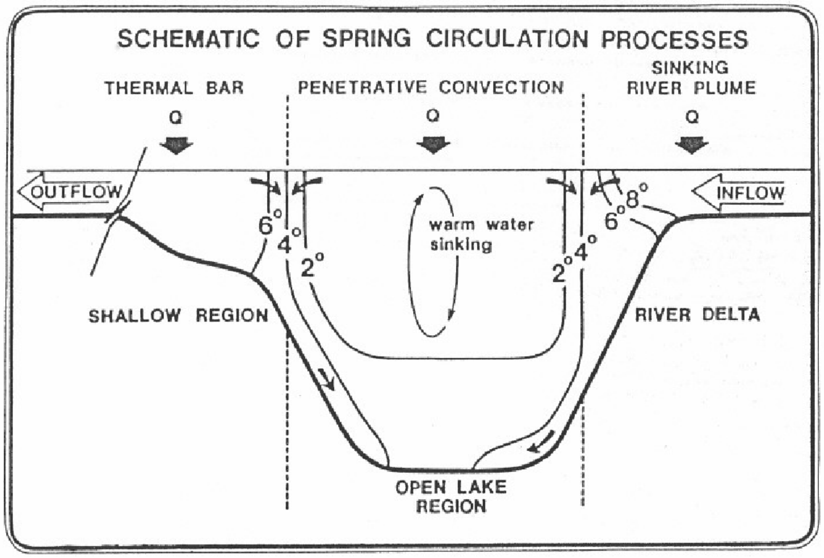

FIG. 14. Schematic illustration of possible spring circulation processes for intermontane lakes.

***Figure 2.6:*** *Schematic of* ***thermal bar*** *- mixing of water slightly above and below 4 °C. In this example, warm inflow water (see surface) meets lake water of 2 °C. The mixture of the two water parcels (in the figure indicated as ~4 °C and slightly warmer) is always heavier than the average of the two original densities (due to non-linearity of the density equation).*

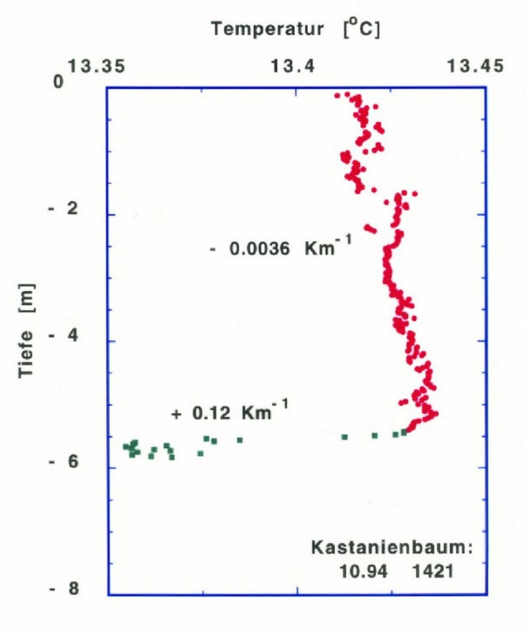

***Figure 2.7*** *Example of a convective surface boundary layer with a slight unstable stratification, due to temperature increasing with depth (taken during night in Lake Lucerne in October). Convective mixing is relatively strong, as temperature with > 13 °C causes high $\alpha$. Temperature differences as small as a few 0.01 °C are typical during convective mixing. For convective plumes: see Figure 2.8.*

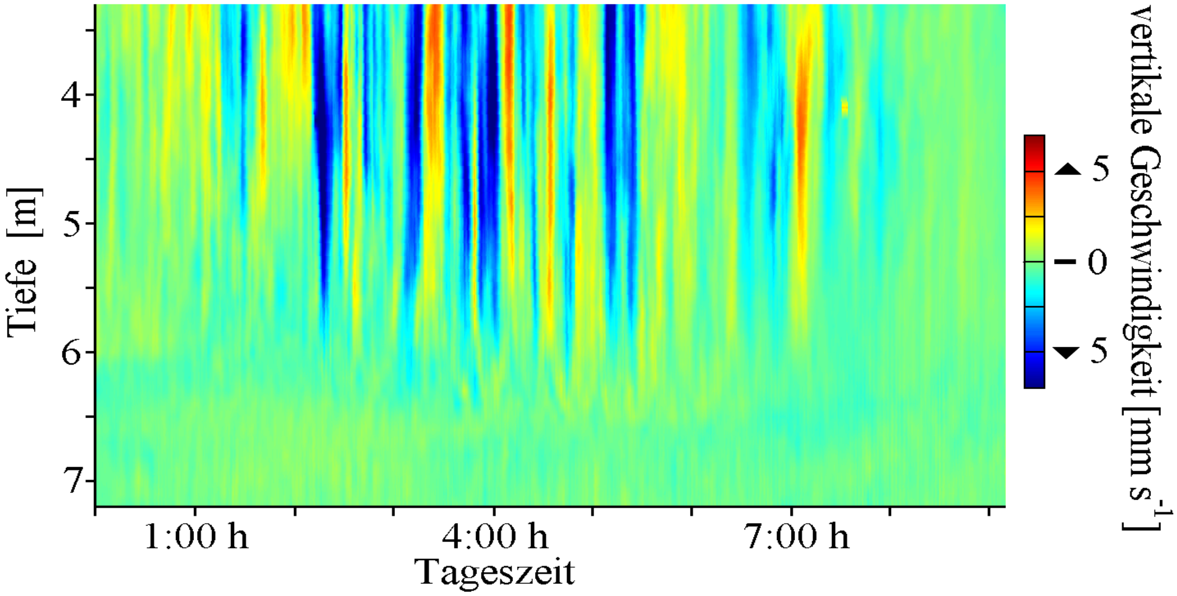

***Figure 2.8*** *Time-series of vertical velocity profiles observed in the top 6 m of the small wind-protected Soppensee during a night of cooling in September. The contour plot reveals a convective surface boundary layer with rising (red) and sinking (blue) convective thermals from midnight to 8 am (~sun rise), while cooling off. The water parcels reach velocities of only ± 5 mm* $s^{-1}$*. Source: Jonas et al. 2003.*

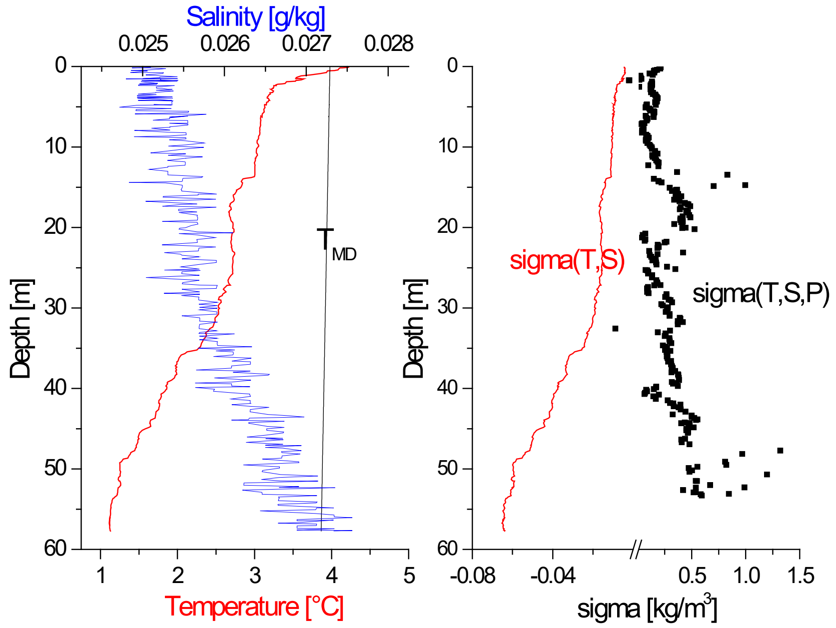

**Figure 2.9** *Example of a stable density stratification caused by particles P in Grimselsee. Density from temperature alone would be unstable (left; T decreasing with depth for $T<T_{MD}$ and therefore at negative $\alpha$) and the salinity gradient is negligible. This situation occurs in glacier lakes / high-alpine reservoirs with high particle concentrations (here about 100 mg $L^{-1}$). Definition of $\sigma = \rho - 1000$ kg $m^{-3}$.*

## References

Apel, J.R., 1990. Principles of ocean physics, London.

Bührer, H. u. Ambühl, H., 1975. Die Einleitung von gereinigtem Abwasser in Seen. Schw. Z. Hydrol. **37**: 372-374.

Chen, C.T. and F.J. Millero, 1986. Precise thermodynamic properties for natural waters covering only the limnological range. *Limnol. Oceanogr.* **31**: 657-662.

Farmer D. 1975. Penetrative convection in the absence of mean shear. Quart. J. R. Met. Soc. **101**: 869-891.

Fujino, K., Lewis, E.L., Perkin, R.G., 1974. The freezing point of sea water at pressure up to 100 bars. J. Geophys. Res. **79**, 1792-1797.

Gruber, N., B. Wehrli, A. Wüest, 2000. The role of biogeochemical cycling for the formation and preservation of varved sediments in Soppensee (Switzerland). Journal of Paleolimnology, **24**: 277-291.

Imboden, D. and Wüest, A. 1995. Mixing mechanisms in lakes. In: Physics and chemistry of lakes (Eds A. Lerman, D. Imboden and J. Gat), pp. 83-138. Springer, Berlin/Heidelberg.

Matzinger, A., R. Pieters, K. I. Ashley, G. A. Lawrence, A. Wüest, 2007. Effects of impoundment on nutrient availability and productivity in lakes, Limnology and Oceanography, **52**, 2629-2640.

Schmid, M., Tietze, K., Halbwachs, M., Lorke, A., McGinnis, D. and Wüest, A. 2004. How hazardous is the gas accumulation in Lake Kivu? Arguments for a risk assessment in light of the Nyiragongo Volcano eruption of 2002. Acta Vulcanologica, **14/15**: 115-121.

Siegert, M. J., J. A. Dowdeswell, M. R. Gorman, and N. F. McIntyre, An inventory of Antarctic sub-glacial lakes, *Antarctic Science* **8**, 281-286, 1996.

UNESCO, 1978. Eighth report on the joint panel on oceanographic tables and standards, Woods Hole, 23±25 May 1977. UNESCO Technical Papers in Marine Science 28.

Wüest, A., G. Piepke and J. D. Halfmann (1996). Combined Effects of Dissolved Solids and Temperature on the Density Stratification of Lake Malawi (East Africa). In Johnson and Odada [eds.] "The Limnology, Climatology and Paleoclimatology of the East African Lakes", *Gordon and Breach Scientific Publishers, New York*, p. 183-202.

Wüest A and E.C. Carmack (2000). A priori estimates of mixing and circulation in the hard-to reach water body of Lake Vostok, *Ocean Modelling* **2**, 29-43.